Mazzei *et al. Chem. Biol. Technol. Agric.* (2024) 11:131
https://doi.org/10.1186/s40538-024-00620-x

Chemical and Biological Technologies in Agriculture

RESEARCH

Open Access

MRI and HR-MAS NMR spectroscopy to correlate structural characteristics and the metabolome of Fiano and Pallagrello grapes with the action of field spray preparation 500 and the soil spatial microvariability

Pierluigi Mazzei[1*], Andrea Sica[1], Claudio Migliaro[1], Gessica Altieri[1], Nicola Funicello[2], Salvatore De Pasquale[2], Alessandro Piccolo[3] and Giuseppe Celano[1]

Abstract

Background A number of Italian grape berry varieties, such as Fiano (F) and Pallagrello Nero (P), represent National strategic products. Therefore, it is important to identify soil conditions emphasizing their peculiar characteristics as well as find innovative and sustainable treatments improving their compositional and nutraceutical quality. The field spray preparation 500 is a biodynamic product that is presumed to serve as biostimulant on the vine. However, so far, the scientific results probing its effectiveness are still lacking. Moreover, it is necessary to establish a reliable relationship between the grape quality and the spatial microvariability of the vineyard's soil. On this basis, the main objective of this work consisted in correlating structural and morphological characteristics (via MRI), the primary metabolome (via semi-solid state HRMAS NMR) and important nutraceutical parameters (total phenols and antioxidants via DPPH assay) of F and P grapes with both the action of preparation 500 biostimulant and the vineyard soil microvariability, based on soil apparent electrical conductivity.

Results HRMAS enabled the identification of the primary metabolome of F and P. The elaboration of ^{1}H NMR spectra through chemometrics revealed significant changes in F and P grapes, accounting for both soil microvariability and the application of field spray (the latter also confirmed by PLS-DA and Heat-map clustering). Interestingly, for both F and P it was observed a significantly lower content of carbohydrates after biostimulant treatment while MRI revealed diagnostic structural and internal details of intact grapes. The combined use of proton parametric indices, such as relaxation times and diffusion coefficients, indicated alterations induced in grapes by both the spatial microvariability of the soil and the effects of investigated biostimulant. Interestingly, a tight correlation was found between MRI transverse relaxation time and the contents in total phenols and antioxidants.

Conclusions Our results have proven that both soil spatial microvariability and the application of field spray preparation 500 significantly affect the structural, metabolomic and nutraceutical characteristics of grapes. Moreover, the preparation 500 treatment has increased the nutraceutical value of grapes. Importantly, these data may be potentially used to promote and protect biodynamic grape and predict the quality of the resulting wines.

*Correspondence:
Pierluigi Mazzei
pmazzei@unisa.it
Full list of author information is available at the end of the article

© The Author(s) 2024. **Open Access** This article is licensed under a Creative Commons Attribution-NonCommercial-NoDerivatives 4.0 International License, which permits any non-commercial use, sharing, distribution and reproduction in any medium or format, as long as you give appropriate credit to the original author(s) and the source, provide a link to the Creative Commons licence, and indicate if you modified the licensed material. You do not have permission under this licence to share adapted material derived from this article or parts of it. The images or other third party material in this article are included in the article's Creative Commons licence, unless indicated otherwise in a credit line to the material. If material is not included in the article's Creative Commons licence and your intended use is not permitted by statutory regulation or exceeds the permitted use, you will need to obtain permission directly from the copyright holder. To view a copy of this licence, visit http://creativecommons.org/licenses/by-nc-nd/4.0/.

Keywords Primary grape metabolome, Proton relaxation times, Diffusion coefficients, Biodynamic, Chemometrics, Antioxidants

Graphical Abstract

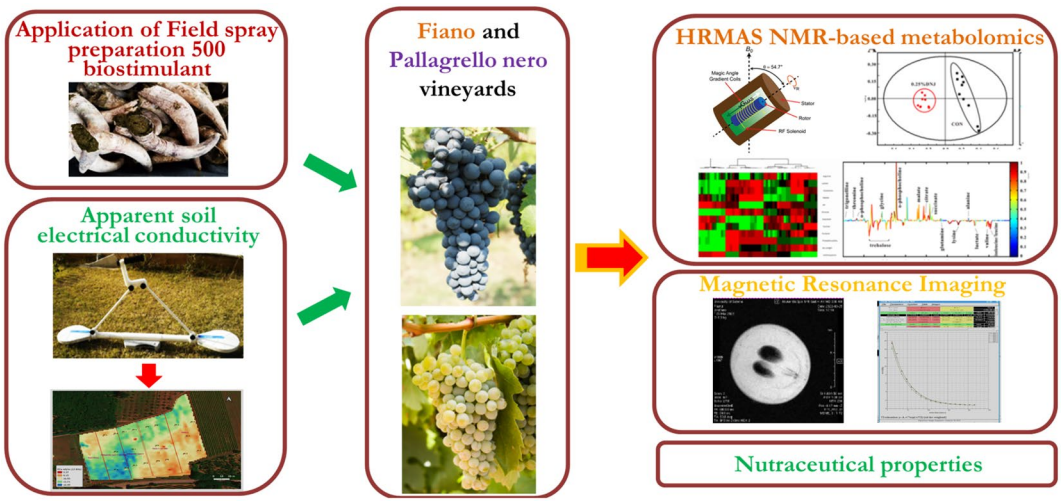

Introduction

About 7.5 million hectares of fertile soils, in the world, are vocated to the cultivation of *Vitis vinifera* and are mostly concentrated in China, Italy, USA, France, Spain and Turkey [1]. Over the 93% of these vineyards is composed by vine cultivars producing quality grapes suitable for the wine industry. Italy represents the second world producer of wine, following the France, with an average production in 2021 of over 50.2 million hecto-liters [2]. From a qualitative point of view, many Italian wines are classified as excellent, as proved by the assignment of 329 D.O.C. (Controlled Designation of Origin) and 70 prestigious D.O.C.G. (Controlled and Guaranteed Designation of Origin) quality labels [3]. A large interest is thus addressed by grape and wine producers towards the identification of innovative agronomic strategies and advantageous soil conditions useful to improve vine productivity and promote the attainment of quality and excellent grapes.

In this perspective, the use of efficient biostimulants can promote vines growth and increase their ability to deal with negative factors affecting their physiology and performances, such as deficiency of soil nutrients and water, pathogens attack and adverse microclimatic conditions. In fact, biostimulants can activate mechanisms eliciting a response in vines, making them more efficient in exploiting soil resources [4–7]. It is noteworthy the fact that effective organic biostimulants may contribute to mitigate the adverse effects due to the incessant onset of climate changes [8]. Biodynamic products, which are obtained in respect of the principles of circular economy and sustainability, may represent suitable candidates for this purpose. For example, it has been proved that the application of a biodynamic treatment on soil and vines may improve grape production and quality, representing an alternative approach to traditional methods often responsible to determine relevant environmental impacts [9, 10]. In particular, the field spray preparation 500 (p500) is an organic product deriving from the biochemical stabilization of cow manure, carried out in respect of biodynamic principles [11]. This product has a complex molecular structure, with an overall low hydrophobic character and composed mostly by aromatic derivatives, polysaccharides, and alkyl compounds [12]. It has been proved that the application of p500 can positively influence the wheat by promoting plant and root growth and increasing the seedling vigor [13]. Recently, a model developed based on proton liquid-state nuclear magnetic resonance (NMR) proves that the molecular composition of grapes, cultivated according to a biodynamic method including the p500 treatment, exhibits a profile significantly different than for grapes resulting from a traditional organic management [14]. However, so far, the literature probing the effectiveness of p500 as biodynamic biostimulant is still poor. Therefore, further

investigations are required to confirm and consolidate the beneficial and effective role of this product.

On the other hand, there is a growing interest related to the use of fast, reliable and georeferenceable methods to better understand the correlations existing between wine quality and the properties characterizing the territory of grape origin. In this context, the electromagnetic induction (EMI) method, typically adopted to conduct precision agriculture, represents a very promising technique allowing the evaluation of soil apparent electrical conductivity (ECa) and its representation through intuitive responsive maps. EMI is very advantageous because permits to predict several soil conditions and properties, such as the content in water, organic matter, active clays and salts, as well as individuate buried rocks at a soil depth which, depending on the selected frequency for the measurement, may explore up to 1.5–2 m [15, 16]. Conceptually, the EMI technique involves the generation of a primary magnetic field, developed from a moving transmitter and oriented towards the soil. The presence of conductive components in soil produces secondary currents that, in turn, develop a secondary induced magnetic field. The detection and the quantification of the latter is finally exploited to extrapolate the soil electrical conductivity [15–17]. Recently, ECa maps have been also used to correlate the spatial variability of soil physical properties with site-specific crop responses, including biological parameters [18] and total soil respiration [19]. It has been found that plant growth parameters, such as height, leaf area index and dry matter, well correlate with soil patterns identified through ECa maps for crops such as winter barley, winter wheat and sugar beet [20]. Similarly, a close relationship between ECa maps and maize plant height has recently been established in field experiments [21]. A significant correlation has been also found between soil microvariability detected via EMI and the molecular quality of Aglianicone grapes in different vintages [22].

On this basis, the purpose of this work was to investigate on the possible effects induced by the p500 treatment on model autochthonous Italian vine cultivars (Pallagrello Nero and Fiano), in open field tests, accounting also for the spatial microvariability of vineyards revealed by EMI method. The influence of both p500 treatment and soil microvariability was verified by examining (i) representative nutraceutical parameters; (ii) the primary metabolome; and (iii) microstructure and morphological traits of studied grapes.

In particular, grape metabolome was unraveled by means of high-resolution magic angle spinning (HRMAS) NMR spectroscopy, in the semi-solid state [23, 24]. This technique permits to obtain NMR spectra through the direct exam of fresh and intact tissues, in a relatively rapid way, with a resolution very similar to that attainable via high-resolution liquid-state NMR [23, 25]. HRMAS represents a very innovative and powerful technique which has been already used with success mostly to investigate on the quality and the origins of relevant agro-food products, such as tomato [26], persimmon [27], sweet pepper [28], and maize [29]. However, despite its undisputable potential, HRMAS is still underutilized, in the fields of food and agricultural chemistry, while it would be useful to explore its unexpressed potential.

The analysis of grape microstructure and morphological traits was carried out by means of magnetic resonance imaging [30–32]. This technique is based on the quantification and the spatial location of water protons and enables the acquisition of detailed morphological images (resolution of tens of micrometers) of internal sections of intact tissues. In addition, the adoption of specific experiments permits to extrapolate multiple and complementary information informing directly on the composition and dynamics of the water molecules in the examined tissue and indirectly on sample microstructure [30, 33]. Up to date, MRI has been used to examine several important aspects of relevant agro-food products, such as tomato [34, 35], radish [36], kiwi [33, 37, 38] and apple [39–41]. MRI is a very powerful imaging technique which so far has been largely used in the medical diagnostics and pharmacological fields. However, similar to HRMAS, MRI potential in the fields of food and agricultural chemistry is still underutilized. Therefore, a further objective of this work was to reveal and demonstrate the suitability and potential role of MRI and HRMAS NMR spectroscopy for investigating on grapes and providing useful information.

Experimental section

Fiano and Pallagrello Nero vineyards and p500 treatment

The grapes of white Fiano (F) and black Pallagrello (P) were produced by the biodynamic farm "I Cacciagalli", located in Teano (Caserta, Italy). Vineyards soil is only few meters shallow, exhibits a slightly acid pH and is characterized by a silty clay texture. F and P grapes were sampled on the 3rd and the 16th of September 2021, respectively, at the full maturation of fruits, which was established on the basis of sugar content (16°Bx for F and 21°Bx for P).

Half of F and P vineyards were treated with field spray preparation 500 (p500), purchased from the association "Agriculture living" and dynamized in the farm immediately before the soil application. The latter occurred in full compliance with the guidelines provided by the Italian association DEMETER. The product was sprayed on the soil on the 1st of December 2020 and 14th of April 2021, using a dose of 250–300 g/ha (Supporting Tab. 1).

The grape samples were collected from plants insisting on soil sites treated (T, treated with 500) and untreated (C, control) with p500. For each cultivar and treatment, at least 100 berries were taken from 5 different plants. Samples were stored at the temperature of − 20 °C until the analysis.

Soil mapping via electromagnetic induction technique

Vineyard's spatial variability was measured by using a multi-frequency EMI sensor (GSSI Profiler EMP-400) equipped with a 1.2 m coil spacing [15, 22].

The measurements were performed on the 16th of September 2020, by setting the vertical dipole mode (VDP), and a frequency of 13 kHz. Such a frequency resulted the best compromise to examine that portion of soil typically explored by the roots of the vine (estimated magnetic field penetration depth of about 1.5 m). ECa values (expressed as mS/m) were obtained by collecting data every 0.75 s, in continuous mode, walking along each row of the vineyard and at a speed of about 4–5 km/h.

The acquisition points were georeferenced using the Tripod Data System Recon Personal Digital Assistant, accompanied by both an integrated Bluetooth service and HoluxTM Wide Area Augmentation System Global Position, with a horizontal dilution of differential correction accuracy. Collected data were then used to develop ECa (apparent electrical conductivity) maps of F and P vineyards. To ensure maximum georeferencing accuracy, the coordinates of the ECa values were determined considering at least 8 satellites. ECa maps were generated by using MagMap2000c and Surfer Golden© and applying the kriging method (single cell 1 × 1 m). Abnormal ECa data acquired in proximity of vineyard metal rollers were removed. Grape berries, for both varieties and as a function of p500 treatment, were sampled by plants insisting on vineyards sites characterized by the highest (H, high, relative range 10.42–14.87 mS/m) and the lowest (L, low, relative range 8.7–11.45 mS/m) ECa values. Specifically, samples were collected at high ECa values (PC3 and PT1, 14.84 and 10.31 ms/m; FC1 and FT1, 12.42 and 13.27 ms/m) and at low ECa values (PC5 and PT1, 11.45 and 10.31 ms/m; FC3 and FT5, 8.7 and 9.55 ms/m) (Fig. 1). For each cultivar, at least 100 berries were taken from 5 different plants. Samples were stored at the temperature of − 20 °C until the analysis. All sample typologies and respective labels are listed in Supporting Tab. 1.

Titratable acidity

For each thesis, 25 grapes were thawed and pressed until to obtain a juice, which was then filtered under vacuum

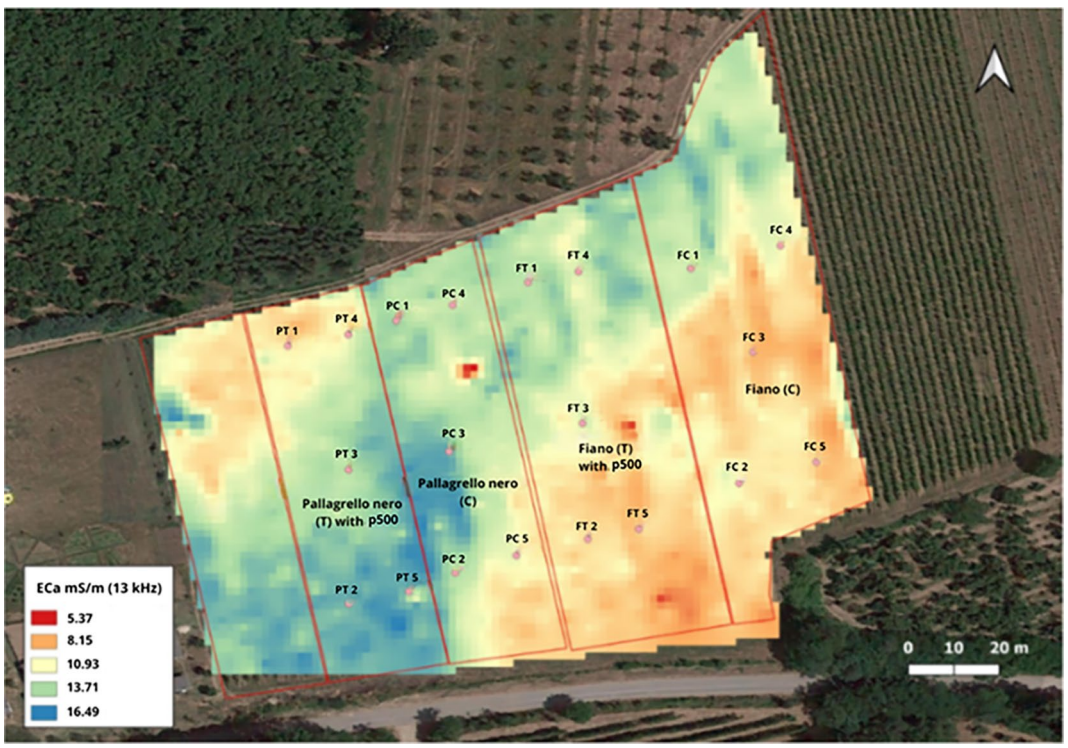

Fig. 1 ECa map of Pallagrello Nero (P, on the left) and Fiano (F, on the right) vineyards obtained by electromagnetic induction technique (13 kHz). The color scale is described in the legend and shifts progressively from red (low ECa values, 5.37 mS/m) to blue (high ECa values 16.49 mS/m) as a function of site-specific electrical conductivity. The image also specify the plots either treated (T) or not (C) with p500

(cellulose acetate filters, Whatman 41, 20 µm pores). Then, a volume of 2 ml of filtered juice was diluted with 98 ml of deionized water, added with phenolphthalein indicator and titrated, under magnetic stirring, with a solution of NaOH 0.1 M. The titratable acidity was expressed as equivalents of tartaric acid (g/l). 3 replicates were analyzed for each grape type.

Grape extraction and quantification of total phenols and antioxidants

For each thesis, 20 grapes were thawed and blended, through an immersion mixer, until the material was completely crushed. Then, 5 g of blended material were put in contact with 20 ml of a 70% (v/v) ethanol solution, ultrasonicated (ARGO LAB DU-32) for 4 min at 30 °C and left under magnetic stirring for 17 h and 30 min, at 4 °C, in absence of light. Afterwards, a centrifugation (10 min at 6000 rpm) was carried out to isolate supernatant which was finally filtered, under vacuum, and stored at the temperature of − 20 °C, until further analyses.

The content in total phenols was determined by using the Folin–Ciocalteu assay and was expressed as gallic acid (GAE) equivalents. The reaction was performed by adding, progressively, 0.2 ml of ethanolic extract, 0.5 ml of Folin–Ciocalteu reagent (diluted 1:3 with bi-distilled water), and 0.5 ml of a Na_2CO_3 solution (10% w/v). After the addition of each component, the mixture was agitated for about 10 s, through a vortex, and held for about 4 min, in absence of light. Finally, the mixture was diluted with 3.9 ml of bi-distilled water and the reaction was left to proceed for 2 h and 30 min, at 25 °C, in absence of light. Each experimental set consisted of 4 replicates and 2 blank samples. For the latter, the volume of grape extract was replaced by the same volume of ethanol 70% solution. The reaction product was examined with a spectrophotometer (Thermo Spectronic 20 Genesys) by setting it at a wavelength of 765 nm. The absorbance values were then converted in GAE through a comparison with a calibration curve, built by launching the reaction with increasing amounts of gallic acid (range 0–1 mg GAE per ml of extract; $r^2 = 0.9804$). The values were expressed in mg of GAE per g of fresh mass.

The antioxidants content was measured by the free radical scavenging assay via DPPH (2,2-diphenyl-1-picrylhydrazyl), and the results were expressed as ascorbic acid (AAE) equivalents. The procedure was carried out by diluting 0.125 ml of extract with 4.325 ml of methanol and adding 0.5 ml of DPPH solution (2.18 mM in MeOH). The mixture was agitated for about 10 s, and then the reaction occurred for 30 min, in absence of light. The results were read with a spectrophotometer (Thermo Spectronic 20 Genesys) at the wavelength of 517 nm. Each experimental set consisted of 4 replicates and 2 blank samples. For the latter, the volume of ethanolic extract was replaced by the same volume of ethanol 70% solution. The absorbance values were then converted in AAE through a comparison with a calibration curve, built by launching the reaction with increasing amounts of ascorbic acid (range 0–960 µg AAE per ml of extract; $r^2 = 0.9938$). The values were expressed in µg of AAE per g of fresh mass.

HRMAS NMR spectroscopy

Per each representative sample, three berries were thawed before HRMAS NMR analysis. After few minutes, each berry was dissected, and few aliquots of grape pulp were sampled per berry. The material was merged and homogenized. About 30 ± 1 mg of homogenized sample was inserted into an HRMAS-NMR rotor (4 mm in zirconia; 50 µl). Few tens of microliters of a phosphate buffer solution (pH 6.8, 0.05 M), prepared entirely with deuterated water (99.8% D_2O/H_2O), were then added to the rotor, by removing possible relatively large air bubbles. The latter was finally closed with a special external cap equipped with fins, serving as turbine and necessary to trigger sample rotation [23, 24].

HRMAS NMR experiments were conducted on a 500 MHz spectrometer (11.7 Tesla, Bruker Oxford spectrospin, Illinois) equipped with a $^1H–^{13}C$ HRMAS probe. The experiments were conducted at a temperature of 22 ± 1 °C, at a rotation rate of 5 kHz and examining at least 4 replicates for grape typology.

^1H NMR spectra were acquired by applying the on-resonance presaturation technique, to suppress the water signal, and setting 16k of acquisition points, 5 s of recycle delay, 8 dummy scans and 256 effective scans. To assign the most intense NMR signals and to support the identification of grapes metabolomic fingerprint [22], 1D proton-decoupled ^{13}C spectra and two-dimensional spectra were also acquired for several representative samples of F and P. The bidimensional spectra consisted in homonuclear $^1H–^1H$ correlation spectroscopy (COSY), total correlation spectroscopy (TOCSY) and nuclear Overhauser effect spectroscopy (NOESY) and heteronuclear $^1H–^{13}C$ heteronuclear single-quantum coherence (HSQC) and heteronuclear multiple-bond coherence (HMBC) [42]. All 2D NMR spectra were set up with 16 dummy scans, 64 scans, 2048 acquisition points for 256 experiments, and spectral windows of 16 and 300 ppm, respectively, for hydrogen and carbon nuclei (in the case of heteronuclear experiments). All spectra were processed (Fourier transform, phase, and baseline corrections) by using Bruker TopSpin software (v. 4.1).

Magnetic resonance imaging (MRI) of grape samples

MRI experiments were performed at a temperature of 25 ± 1 °C on a wide-bore Bruker Avance 300 MHz magnet (Bruker Isospin, Rheinstetten, Germany), equipped with a μ-imaging MICRO 5 probe and operating at a proton frequency of 300.13 MHz. For each analysis, one grape berry was loaded into a sterilized 25 mm tube (Norell, borosilicate). An inert and soft material was put on the bottom and on the top of the tube to stabilize vertically the grape, during the analysis, and avoid the possible interference of water exuded from grape. Then, each tube was tightly closed to minimize the grape water evaporation (Supporting Fig. S1).

Three types of MRI experiments were launched to identify longitudinal spin–lattice (T_1) and transverse spin–spin (T_2) relaxation times as well as self-diffusion coefficients (DIFF), respectively. T_2 experiments were acquired by applying a multi-slice–multi-echo pulse sequence, setting a recycle delay of 6 s, 4 scans and 18 sub-experiments, each of them characterized by an increasing number of spin–echoes (the total spin–echo duration varied gradually and progressively from 12 to 216 ms, in 18 experiments) [30–32]. The data were fitted according to the following equation:

$$M_t = M_0 \exp(-t/T_2), \tag{1}$$

where M_0 and M_t represent the resulting magnetization intensity at the minimum spin–echo delay and after the *i*th spin–echo interval, respectively. The 2D images extrapolated from this experiment, at the shortest spin–echo duration (12 ms), was exploited for morphological evaluations.

T_1 experiments were acquired by applying an inversion recovery pulse sequence and performing experiments at increasing repetition times, which gradually varied from 700 to 7500 ms. The experiments were set with an echo time of 65 ms and 4 scans. The data were fitted according to the following equation:

$$M_t = M_0[1 - \exp(-t/T_1)], \tag{2}$$

where M_0 and M_t represent the resulting magnetization intensity at the minimum repetition time and after the *i*th delay, respectively.

The self-diffusion coefficients (DIFF) were extrapolated from a pulse sequence based on the use of pulsed field gradients and integrated with stimulated echoes. The experiment was set with a recycle delay of 6 s, 6 scans, a delay of 4 ms for the two gradients (δ, little delta), 13 ms as interval (Δ, big delta) between the first (encoding) and second (decoding) gradient. The strength of gradients increased progressively (100, 400, 750, 1000, 1500, 2168 s mm^{-2}) in 6 experiments. The data were fitted according to the following equation:

$$M_t = M_0 \exp\left[-\gamma^2 G^2 \delta^2 (\Delta - \delta/3)\, D\right], \tag{3}$$

where M_0 and M_t represent the resulting magnetization intensities after the application of the weakest gradient and that at the *i*th strength, respectively, γ is the gyromagnetic ratio of hydrogen, G is the intensity of the pulsed field, δ is the duration of the gradient, and Δ is the time interval between the first (encoding) and second (decoding) gradient.

All MRI images resulted from the acquisition of 6 interlaced axial slices, with a thickness of 1 mm, a visual window of 18 × 18 mm^2 (Supporting Fig. S2, on the left). The images consisted of a matrix 256 × 256 for T_1 and T_2 experiments and a matrix 128 × 128 for DIFF experiments.

Bruker's Paravision 6.0.1 software was used to process MRI data, obtain images and perform the data fittings. Calculations for the fittings were carried out by examining and averaging, per sample, 12 regions of interest (ROI) distributed over 4 slices. Briefly, 4 representative slices, per sample, were considered and, for each of them, 3 circular ROIs (area ≈0.4 cm^2; Supporting Fig. S2, on the right) were selected (3 ROIs × 4 slices × sample). At least 4 replicates were acquired for each type of grape.

Multivariate analysis

For each replicate, all HRMAS NMR proton signals included in the spectral range 7.766–0.764 ppm were assigned and integrated by creating buckets with variable width and sized to include whole peaks (either singlets or multiplets, depending on compound structure). For each grape variety (F and P), it was produced a data matrix composed of 43 variables (integrations) per a total number of observations accounting for both p500 treatment (Control vs Treatment), and the ECa values (L vs H) of soil sites (at least 4 replicates per sample typology).

For each ^{1}H NMR spectrum, the area corresponding to each single integration was normalized, with respect to the sum of the individual areas (expressed in %), and Pareto-scaled to prevent the underestimation of relatively low intense NMR signals [43, 44]. The F and P matrixes (either whole spectrum or containing only significant variables, depending on the elaboration phase) were elaborated through multivariate statistic techniques. Principal component analysis (PCA) was used to identify the variables (loading-vectors) discriminating different grape types. The ANalysis Of VAriance (ANOVA) test was applied to assess the significance (Tukey and Benjamini–Hochberg FDR tests, both set at an α confidence level of 0.05) by which the most relevant variables (extrapolated through the evaluation of PCA loading-plots) contributed to differentiate the composition of grape types [43, 44].

Heat-map variable analysis and partial least square discriminant analysis (PLS-DA) were applied by considering the variables significantly involved in the discrimination among the samples. For Heat-map clustering, the values were centered, reduced and displayed as colors ranging from red (relatively higher) to yellow (relatively lower) through orange (intermediate values). Samples were clustered using Euclidean's distance. PLS-DA permitted to assess the ability to objectively and significantly (α confidence level of 0.05) discriminate the composition of different grapes by providing the % of correct sample classification, and the receiver operator characteristics (ROC) curve [43]. It was also performed a cross-validation (CV) session based on the PLS-DA test. In particular, the method consisted in building a validation set, achieved by dividing all samples in either a training (discriminant model composed by samples which had been classified a priori) or a test (cross-validation composed by unclassified samples) set. The distribution of samples into the two different sets was conducted accounting for the number of replicates per sample type and aimed to maintain a number of replicates in the training set > 70%. This validation was repeated 5 times by randomly inverting, per each grape type, the samples included in the training and test sets. The larger the percentage of correct classification of test set samples, the better the discrimination extent among of samples. One representative score-plot, out of the five obtained, was shown for P and F PLS-DA cross-validations [43].

The values resulting from MRI experiments (T_1, T_2 and DIFF) were subjected to the analysis of variance (ANOVA) statistical test to verify the significance (Tukey and Benjamini–Hochberg FDR tests, both set at an α confidence level of 0.05) by which the variables contributed to differentiate the different types of grapes.

PCA, ANOVA, PLS-DA and Heat-map tests were carried out by the XLStat software (v.2019, Addinsoft, Paris, France).

Results and discussion

HRMAS NMR spectroscopy

Semi-solid state HRMAS NMR spectroscopy represents a very innovative and powerful technique which, despite its undisputable potential, is still underutilized in the fields of food and agricultural chemistry. HRMAS permits to obtain NMR spectra by the direct exam of fresh and intact tissues, relatively rapidly and with a resolution very similar to that attainable via NMR in liquid-state and high resolution [24, 25]. On this basis, such a technique was exploited to identify the primary metaboloma of Fiano and Pallagrello Nero grapes and research possible correlations with both soil electrical conductivity and the treatment based on the biodynamic preparation 500 biostimulant.

Initially, the most appropriate rotor spin rate was established. In fact, if, on one hand, the NMR spectral resolution of a sample analyzed in the semi-solid state can be improved by increasing the spin-rate, on the other hand, an excessively high rotational speed can alter the integrity of the sample, penalizing reliability, spectral quality and reproducibility [24, 25]. Therefore, through a preliminary set of tests, we found that the best compromise consisted in a spin rate of 5 kHz.

Different regions of the ^{1}H HRMAS NMR spectrum of a representative F berry is shown in Fig. 2. The identification of the most intense proton signals found in both grapes types permitted to define their primary metaboloma [4, 22, 44–46]. Figure 2 reports the assignment of the main proton signals detected, almost exclusively, in the two regions of alkyl (0.5–2.5 ppm) and hydroxyalkyl (2.5–5.5 ppm) protons. Most of predominant signals were attributed to multiplets in carbohydrates such as glucose, fructose and sucrose, followed by xylose but with a content significantly lower. Several amino acids were found in P and F berries, and consisted in proline, asparagine, GABA, glutamate, arginine, lysine, alanine, threonine, and valine. The metabolomic profile was also composed by alcohols, like methanol and ethanol, organic acids, such as tartaric, succinic and malic acids, and other compounds such as choline and lipid molecules (broadened signals in the alkyl region). Except for very weak and broadened signals, which were attributed to tryptophan and phenylalanine, there were no relevant peaks and multiplets at low field frequencies, and, in particular, in the aromatic region. This was explained by the fact that the examined tissue consisted in grape mesocarp, which notoriously lacks of phenolic and polyphenolic compounds (i.e., tannins and anthocyanins). In fact, the latter ones are expected to be much more concentrated in the grape skin and pips. The profile of the primary metabolome of F and G grapes was thus defined and, from a qualitative point of view, the same compounds were detected in both grape varieties. Subsequently, a semiquantitative comparison among the integrations of F and G spectra was conducted aiming to find significant, objective, and diagnostic characteristics related to both the soil spatial variability (based on ECa values detected via EMI technique) and the action exerted by the p500 application. It is important to underline that the studied grapes were harvested in the same vintage (September 2021), from the same vineyards and the same type of soil, managed by the same producer, and grown in the same microclimatic conditions.

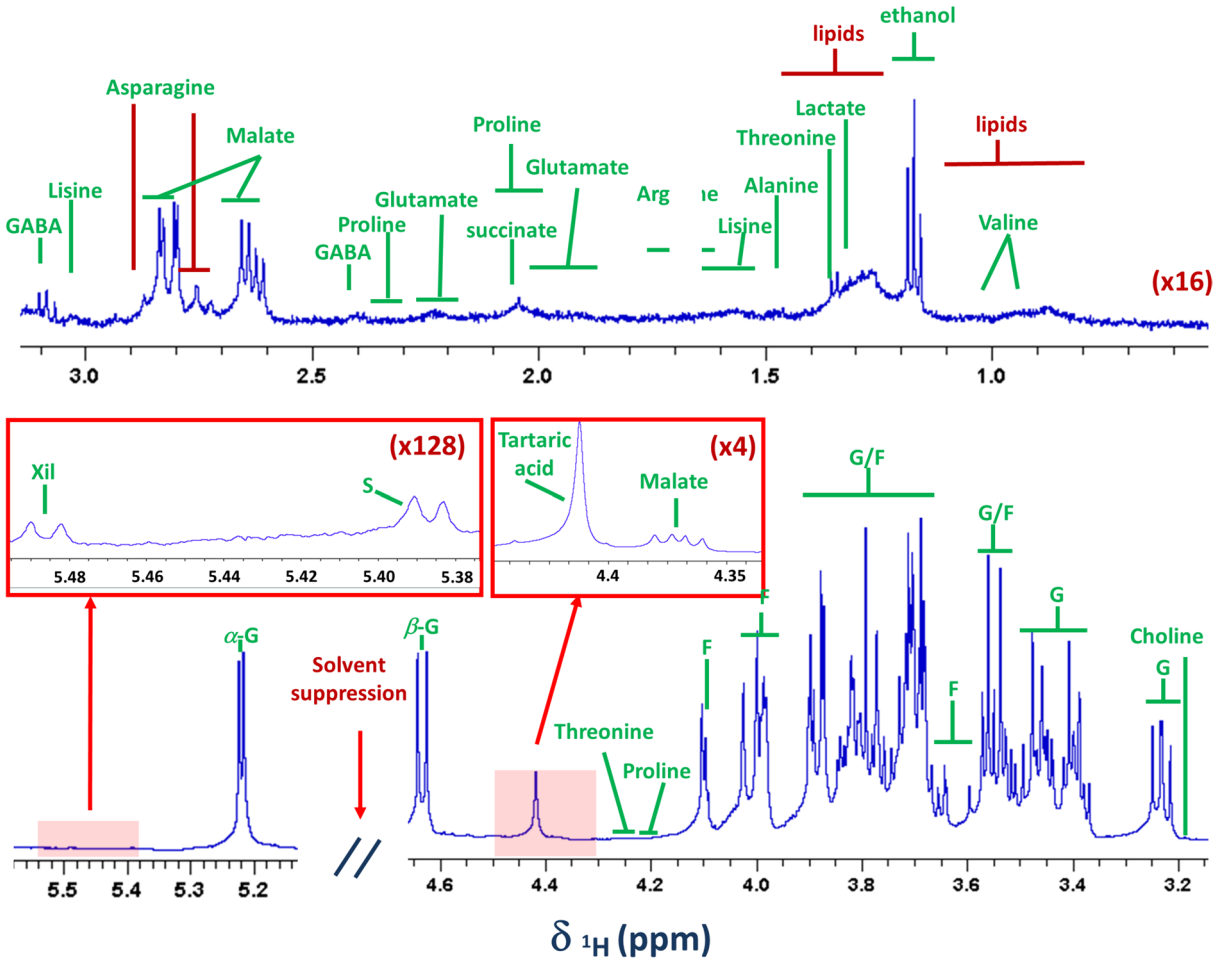

Fig. 2 ^{1}H HRMAS NMR spectrum of a representative sample of PALLAGRELLO grape berry. The figure reports an expansion and magnification (entity of magnification is reported in parentheses) of the following spectral regions: 0.4–3.1 ppm (×16); 3.2–4.8 ppm; 5–5.6 ppm. Red boxes include an additional magnification of the regions 5.26–5.52 ppm (×128) and 4.35–4.55 ppm (×4). The figure reports the name of compounds attributed to the signals. The abbreviations G, F, S and Xil refer to carbohydrates glucose, fructose, sucrose and xylose, respectively

Soil spatial microvariability

In order to correlate soil vineyard microvariability with the primary metabolome of studied grapes, we elaborated the integrations of their HRMAS NMR spectra via principal component analysis (PCA). The latter is an unsupervised multivariate statistical analysis enabling the rapid identification of statistical groups of observations characterized by specific peculiarities. It allows an effective exploration of very large data matrices, providing, in a single output (namely score plot), clear information on systematic variations induced by specific conditions and/or treatments, and revealing, at the same time, the variables responsible for these discriminations [43]. Therefore, ^{1}H NMR HRMAS spectra of F samples collected from plants located in the soil sites characterized by a low (L, 9 mS/m) or high (H, 13 mS/m) ECa responses were thoroughly compared via PCA. Figure 3a, b shows both the PCA score-plots and the most significant spectral comparisons between Fiano samples, for both control and p500-treated plants. The score-plot displayed in Fig. 3a refers to FC samples and results from the linear combination of the line PC1 and PC2, explaining 44.18 and 24.03% of total system variability, respectively. The fact that both L and H groups were placed in markedly different regions of the score-plot, indicated neat and peculiar differences in their primary metabolomas. Firstly, the metabolites mostly representing the PC1 and PC2 were individuated by examining the respective PCA loading-plot. Then, the metabolites responsible to significantly discriminate L from H were selected via ANOVA test. FC collected in L sites exhibited a lower content in amino acids, such as proline, glutamate, GABA, alanine, valine, and threonine, associated with a lower content in ethanol and lipids (differentiation expressed along the PC1). Also the lower content in xylose permitted a collocation of L samples at higher PC2 values, thus

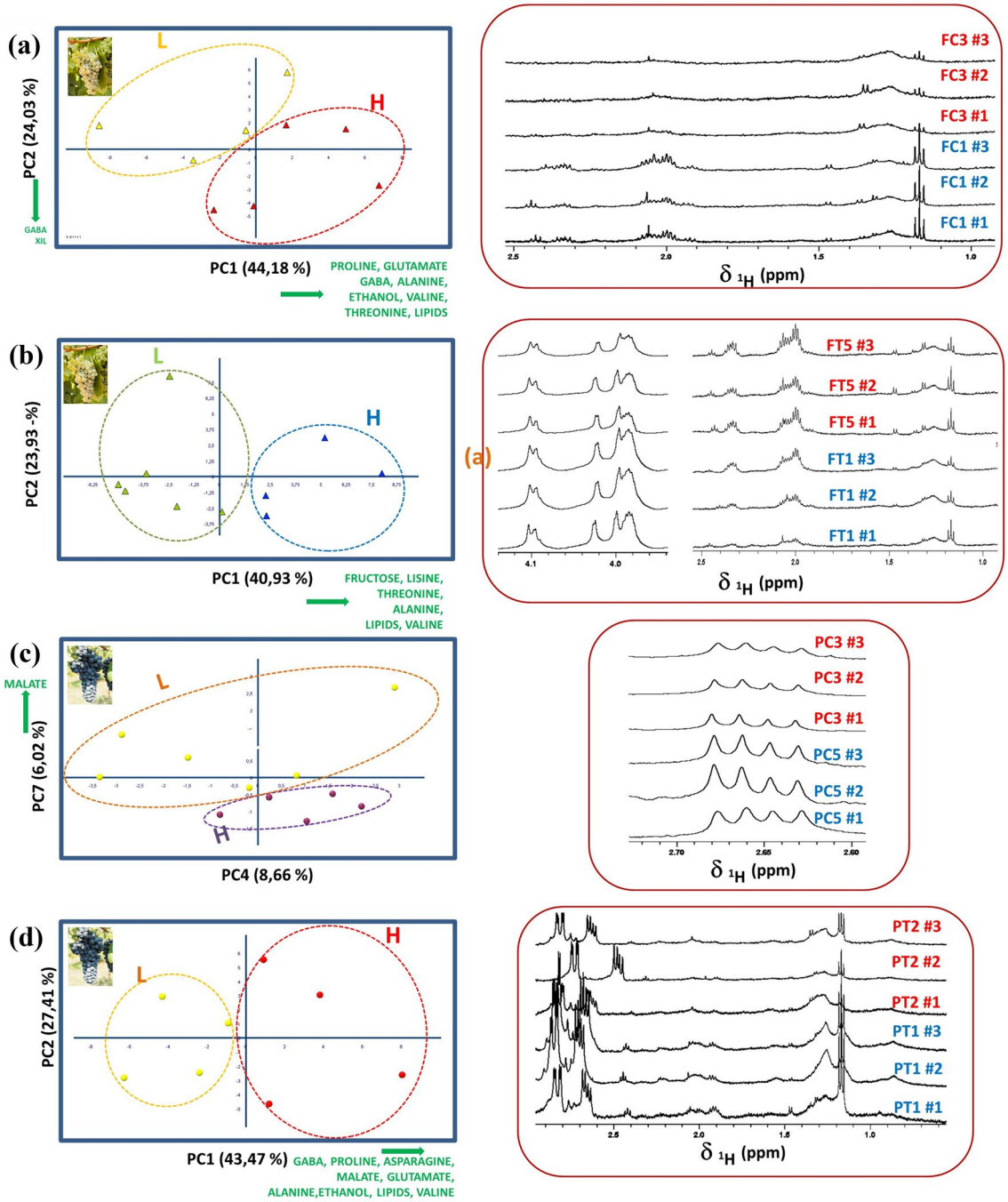

Fig. 3 PCA score-plot obtained by comparing ^{1}H HRMAS NMR spectra of Fiano (F) and Pallagrello (P) mesocarp tissues, sampled from vineyard sites characterized by high (H) and low (L) ECa values, and collected from plants untreated (**a**, **c**) and treated with the biostimulant p500 (**b**, **d**). In green, along the edges of score-plots, are reported the name and the orthogonal direction of the most significant loading vectors responsible for the discrimination between the compared types. On the right side of each score-plot they are shown the NMR peaks mostly involved in the discrimination between the grape types (3 replicates # per type)

contributing to the discrimination. On the right-side of Fig. 3a it is exhibited a comparison among the spectral regions (3 replicates per grape type) including the NMR signals mostly involved in the discrimination between the two types of grapes.

Figure 3b reports a comparison between L and H Fiano samples resulting from treatment with biodynamic

p500. Again, the combination of PC1 and PC2 (respectively, 40.93 and 23.93% of the total explained variability) implied a clear differentiation between FT_L and FT_H. The discrimination occurred only along the PC1 and was due to the fact that FT_H samples exhibited a higher content in fructose, lysine, lipids, and valine, accompanied by a lower amount of GABA, threonine, and alanine. Again, the spectral comparison in the right-side of the figure highlights the neat semiquantitative differences between the two types of grapes. These results proved that, in all cases, the metabolome of F samples changed significantly, as a function of soil electrical conductivity, thus proving that the factors which determined a difference of 4 mS/m between the ECa values of L and H sites are sufficient to affect the vine metabolism.

The score-plot exhibited in Fig. 3c informs on the metabolome of Pallagrello grapes (untreated with p500) as a function of different ECa responses. Only the combination PC4 and PC7 (explaining the 14.68% of total variability) allowed a discrimination between H and L, and was exclusively due to a significantly higher content of malic acid in PC_L samples.

In case of P samples treated with the biostimulant p500, it was detected a neat discrimination as a function of soil ECa responses (Fig. 3d). The discrimination occurred by combining the PC1 (43.47%) with the PC2 (27.41%) and was ascribed to the higher content in GABA, proline, asparagine, malate, glutamate, alanine, ethanol, lipids, and valine in PT_H samples. Interestingly and in agreement with the results concerning F berries treated with p500 (Fig. 3b), also in PT samples it was recorded an over-expression of several amino acids. Another common aspect is that valine and lipid compounds resulted higher than in L, for both FT_H and PT_H. Also for P grapes, the different ECa values revealed soil sites with different characteristics and affecting differently the grape metabolism.

The soil spatial variability identified by EMI technique is mainly attributable to the overall distribution in active clays, water, and organic matter which contribute to increase the apparent electrical conductivity [16]. Our results, based on sites with ECa values at least of 8 mS/m and characterized by an average difference of 4 mS/m, proved that investigated soil sites experimented specific soil conditions which, not only were indirectly revealed by EMI, but also significantly impacted on both vine physiology and grape metaboloma. In fact, in all of studied cases, it was verified that at different ECa values corresponded systematically a different metaboloma. In addition, such a discrimination resulted even more pronounced for samples subjected to biostimulant treatment. Interestingly, this outcoming well agrees with a recent paper focusing on Aglianicone black grapes [22] and proving the existence of a tight and systematic correlations between the composition of Aglianicone grapes, revealed via HRMAS NMR, and ECa soil data.

Effects induced by p500 treatment on grape metabolome

PCA was also exploited to investigate on possible effects induced by the action of the biostimulant p500 on the composition of the two varieties of grapes F (Fig. 4a) and P (Fig. 4b). Interestingly, both varieties of grapes showed an enhanced p500-dependent change in the primary metaboloma. The score-plot differentiating FC from FT grapes was obtained by combining PC1 and PC2 (56.67% of the total system variability explained; Fig. 4a). The discrimination occurred along the bisector direction between the second and the fourth quadrant and was determined by a higher content in proline, glutamate, GABA, alanine, ethanol, and lipids, in samples resulting from p500 treatment, accompanied by a lower content in sucrose and fructose. For P samples, the neat differentiation occurred along the PC1 (48% of the total variability of the system; Fig. 4b). Analysis of the loading-plot, combined with the ANOVA test, revealed that the PC samples exhibited a significantly lower content in metabolites such as glucose, fructose, proline, glutamate, lysine, alanine, threonine, and lipids.

These outcomes suggest that, for both P and F grapes, the p500 treatment may promote the expression of several amino acids as well as can impact on carbohydrates contents. As compared to the control, the p500 induced an increase of proline, glutamate and lipids for both FT and PT. However, the influence induced by p500 on vine metabolism seems to vary as a function of the variety. A certain influence of biodynamic products on the expression of amino acids have been already observed previously. For example, Picone and coworkers [14], in agreement with our results on FT, have demonstrated that the concentration of GABA, in treated grapes, was significantly higher than the grapes subjected to traditional organic treatment, as well as it was proved that biodynamic treatments positively elicited the production of isoleucine and valine [47].

Heatmap (Fig. 5) not only confirmed the discriminability of explored samples, by clusterizing control and p500 samples into two distinct groups for both P and F samples, but also highlighted, in a direct and simple way, the semiquantitative response (red to yellow scale) of the variables significantly involved in the grape type discrimination. In case of F samples, the map underlined a lower content in sucrose and fructose in FT samples, accompanied by a larger amount of glutamate, proline, lipids, alanine ethanol and GABA (Fig. 5a). In case of Pallagrello grapes, the heat map confirmed the pronounced difference in the primary metabolome induced

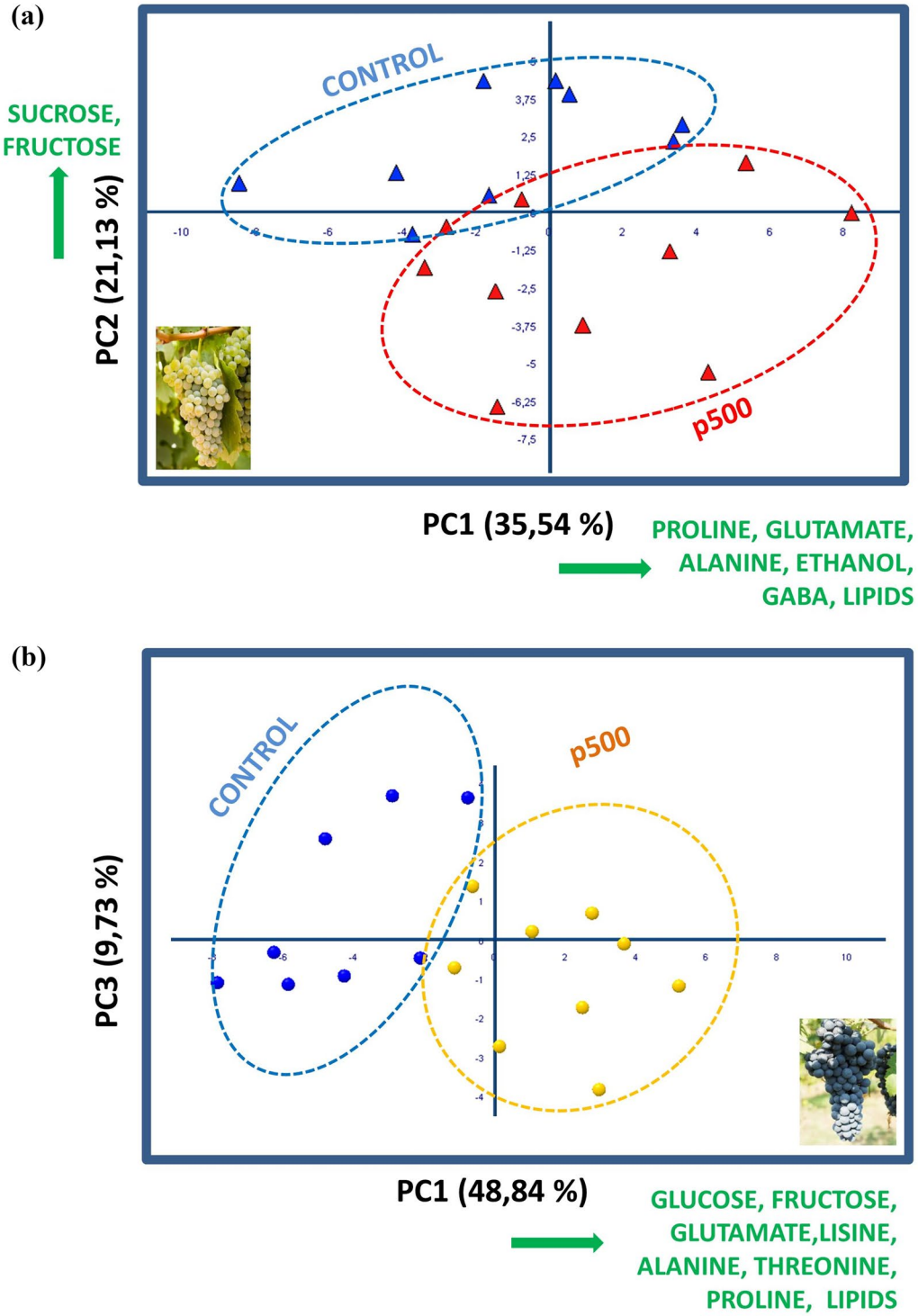

Fig. 4 PCA score-plot obtained by comparing ^{1}H HRMAS NMR spectra of Fiano (F, **a**) and Pallagrello (P, **b**) mesocarp untreated (Control) and treated with p500 (p500). In green, along the edges, are reported the name and the orthogonal direction of the most significant loading vectors responsible for the discrimination between the compared types

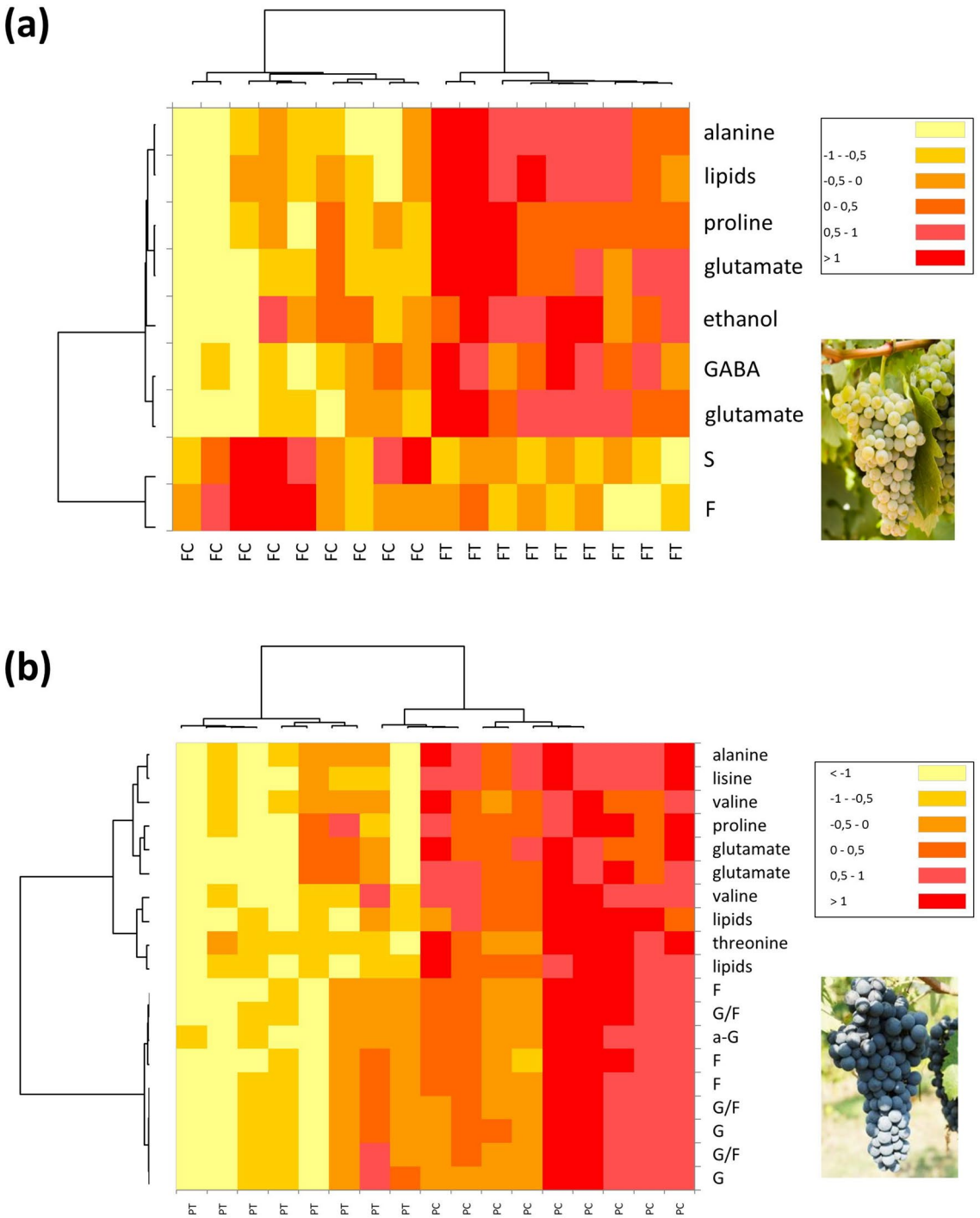

Fig. 5 Heatmap of Fiano (F, **a**) and Pallagrello (P, **b**) grapes untreated (C) and treated (T) with p500. The values for variables were centered, reduced and displayed (see legend) as colors ranging from red (relatively higher) to yellow (relatively lower) through orange (intermediate values). Both samples and variables were clustered by applying the Euclidean's distance. G, a-G, F and S refer to glucose, alfa-glucose, fructose and sucrose, respectively. Several metabolite were cited more than once when more than one NMR signal contributed to heat map clusterization

by p500 treatment. In fact, most of PT samples exhibited a higher abundance of fructose and glucose, as well as a higher expression of several compounds, including amino acids and lipids. Finally, it was applied the cross-validation test of PLS-DA to further prove the capacity of the used analytical approach to discriminate control from

p500-treated Fiano and Pallagrello grapes in a reliable way. The test was successful since in each of five cross-validations, the "unknown" replicates were classified correctly at the 100%. In Supporting Fig. S3 are reported the outputs of one representative cross-validation test for both Fiano (Supporting Fig. S3a–c) and Pallagrello grapes (Supporting Fig. S3d–f). The figure includes the PLS-DA cross-validation score-plot, the PLS-DA receiver operator characteristics (ROC) curve in which the area under the curve corresponded to 1 and the PLS-DA cross-validation results. In conclusion, these outcomes showed unequivocally that biostimulant preparation 500, when applied with appropriate times, methods, and amounts, can influence the primary metabolism of vines, with effects which reflect on the berry composition and with possible implications on grape and wine quality. This finding is very important because permits to candidate the proposed HRMAS-based metabolomic approach as a reliable tool to prove objectively the biodynamic nature of the product, thus permitting to protect biodynamic producers as well as permit them to valorize and promote their products.

Titratable acidity, contents in total phenols and antioxidant agents

The titratable acidity of grape is an important parameter because is related to the pH, accounts for content in weak acids, impacts on organoleptic properties and influences the winemaking process. It is mostly influenced by predominant organic acids which are represented by tartaric acid (0.2–1.0%, on fresh weight), followed by malic, succinic and citric acid [48]. It is reported that the content of tartaric acid, generally ranging between 3 and 9 g/l, depends on the variety, production area, vintage, and terroir [14, 48–51].

F grapes exhibited a significantly higher titratable acidity than the P one (Table 1). This was expected, due to the fact that the pH of white grape berries is typically more acid than the red ones. Moreover, samples FT_L, PT_H and PT_L showed the highest values for F and P variety, respectively. Importantly, all of these samples resulted from the p500 treatment, thus suggesting a possible role of this biostimulant in eliciting an accumulation of organic acids in grapes. The titratable acidity did not vary among P samples, with an average value of 3.86 g/l. Conversely, this parameter varied markedly among F samples, as a function of both p500 treatment and soil ECa values. In detail, FT_L was characterized by the highest titratable acidity, which corresponded to 5.62 g/l. Interestingly, the slightly but significantly higher titratable acidity of PC_L than PC_H is in line with the highest content in malic acid for PC_L already observed by HRMAS NMR.

The content in total phenols was evaluated in all investigated grapes through the Folin–Ciocalteu assay. As expected, the black grape berries P exhibited significantly higher contents in total phenols than the white berries F, with average values of 1.455 and 0.655 mg GAE/g FW, respectively. These values are in line with the content in total phenols for red grapes, which generally ranges within 1.2 and 3.35 mg GAE/g FW, while, for white berries, the range is typically included between 0.32 and 2 mg GAE/g FW [52–55]. The highest contents in total phenols were observed for F and P grapes treated with p500, as compared to the respective control (Fig. 6). The assumption of food rich in total phenols is important due to the beneficial properties of these compounds. In fact, they may serve as powerful antioxidants, prevent inflammations, stimulate positively the nervous system, prevent cardiovascular diseases and seem to be related to anti-tumor activity [56]. On this basis, it is possible to conclude that the application of biodynamic treatment not only influenced the primary metabolome of F and P grapes, but also implied an increase in their nutraceutical and healthy value.

In addition, it was found also a neat correlation between the phenols content and site-specific ECa responses. In fact, except for FT_H and FT_L which did not vary at all among each other, FC_L was significantly higher than FC_H. Conversely, in case of Pallagrello samples, the total phenols responses changed significantly, as a function of ECa values, by exhibiting the highest contents in case of PC_H and PT_L (Fig. 6b).

The DPPH assay was carried out to quantify the free radical scavenging activity in studied grapes. It was detected a significant amount of antioxidants in both varieties (Fig. 6c, d) with higher average values for P grapes. While the differences in antioxidants for P types were very small, although significant, a more enhanced

Table 1 Titratable acidity (g/l of tartaric acid equivalents) of Fiano (F) and Pallagrello Nero (P) grape berries, collected from soil sites characterized by low (L) and high (H) ECa levels, and treated (T) or not (C) with p500

	PC_H	PC_L	PT_H	PT_L	FC_H	FC_L	FT_H	FT_L
Titratable acidity	3.78 ± 0.002 (f)	3.81 ± 0.001 (f)	3.93 ± 0.0001 (e)	3.93 ± 0.0009 (e)	5.50 ± 0.02 (b)	5.04 ± 0.008 (c)	4.87 ± 0.0009 (d)	5.62 ± 0.0009 (a)

The results are expressed as average of 3 replicates and are associated to standard deviation. The letters in parantheses indicate the ANOVA results, where different letters refer to significant differences ($p<0.001$)

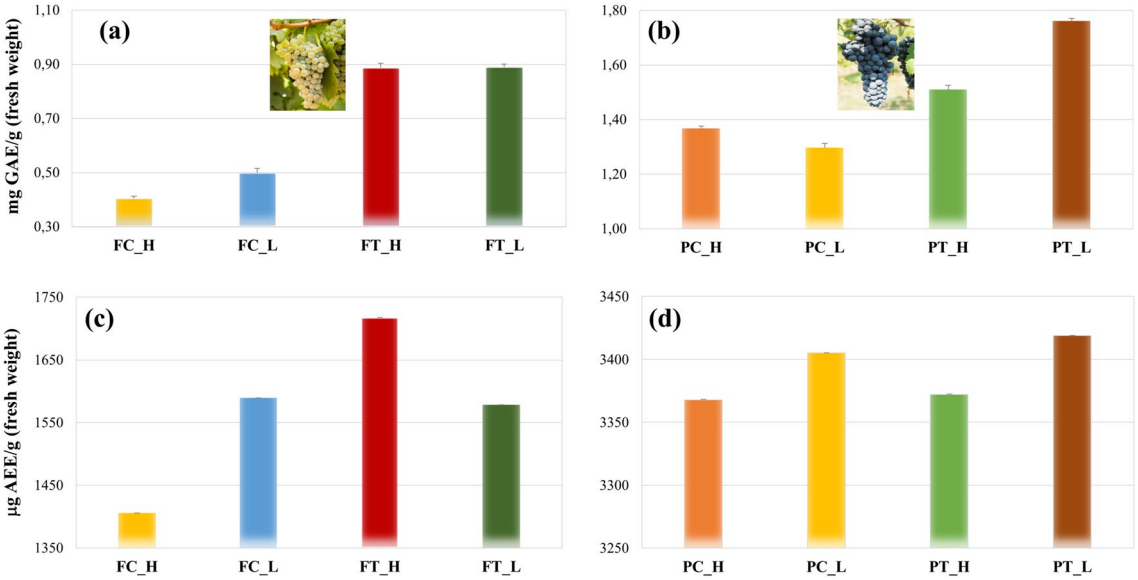

Fig. 6 Contents in total phenols (up, mg GAE/g FW) and antioxidants (down, µg AAE/g FW) of Fiano (F, on the left; **a**, **c**) and Pallagrello Nero (P, on the right; **b**, **d**) grapes. The bars on the top of each histogram represent the respective standard deviations. The labels L, H, C and T refer to low soil ECa levels, high soil ECa levels, control and p500 treatment, respectively

difference was observed for F grapes. Part of these responses well agrees with the results observed for the total phenols, since most of the antioxidant activity deriving from the assumption of grapes, is actually ascribable to phenolic and polyphenolic compounds. The antioxidant activity in red grape berries ranges between 2244 and 3154 µg of AEE/g FW [56, 57], while the average content of antioxidant agents in white berried grapes typically is included within 1233 and 1408 µg of AEE/g FW. Again, in agreement with the total phenols, the samples FT_H and PT_L, both resulting from the treatment with the biodynamic product, gave, in absolute, the highest responses in antioxidant activity, with values of approximately 1718 and 3419 µg AAE/g FW, respectively. These results were even higher than those typical for red and white berries. About the correlation with ECa vineyard responses, in case of Pallagrello the values varied slightly, as a function of ECa values, with L samples giving the relatively higher values. In case of Fiano grapes, the changes ascribable to site-specific ECa values, were much more pronounced, with the highest values observed for FC_L and FT_H.

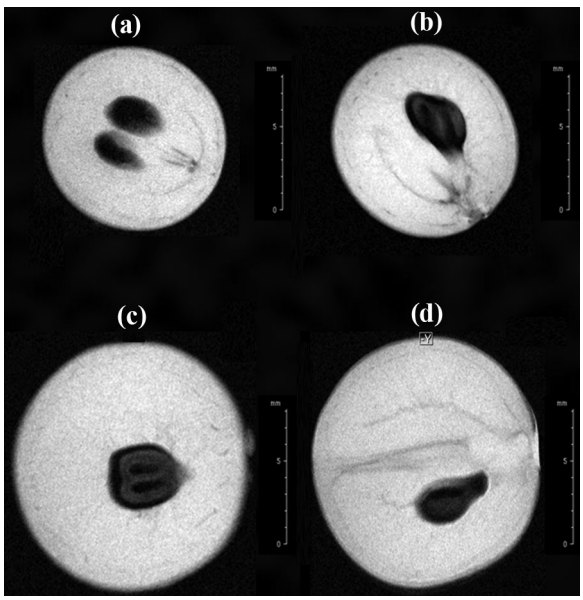

Fig. 7 Spin-density images of two different slices of representative Fiano (**a**, **b**) and Pallagrello Nero (**c**, **d**) grapes. The images were obtained by setting a total spin–echo duration of 12 ms

MRI analysis of Fiano and Pallagrello grape berries

MRI was exploited to examine the inner morphology of intact berries of Fiano and Pallagrello cultivars. In Fig. 7 are shown the MRI images related to the central slices of representative Fiano (a) and Pallagrello Nero (b) grape berries. MRI images clearly permitted to distinguish the three main morphological tissues composing this fruit. In fact, the thin outer darker layer is composed by the exocarp and the epidermis, whereas the mesocarp corresponds to the large area occupied by intense and whitish signals due to the high water content. The seeds are neatly identifiable in the endocarp by the presence of dark semi-ellipsoidal areas, characterized by a relatively darker and

external area (the tegument) and relatively greyish and lighter area (the endosperm contained in the seeds). The latter ones appear significantly darker than the surrounding mesocarp tissue being poorer in water and richer in oils and polyphenols. Furthermore, it was also possible to appreciate the vascular system and, in particular, the peripheral vascular bundles, branching out in proximity of the exocarp, the central fibrovascular bundles, developing below the cercine, and the bundles directly connected to the seeds (Fig. 7; supporting videos 1 and 2). These images suggest that MRI can reveal anatomical details of intact in vivo or ex vivo samples, with a resolution of tens of microns. This is important because paves the way to its use to investigate on the early detection of treatment-related effects on inner grape morphological traits. It is important to underline that, to date, only one research group [58] has successfully attempted to use MRI to investigate on grape berries, by detecting interesting effects exerted on Nero di Troia grapes as a function of different fertilizers. Although this further proves the potential role of MRI in studying grapes, on the other hand, it certifies how the MRI potential to examine grape is still largely unexpressed and unexplored, thus requiring further validations.

Firstly, MRI images of F and P were accurately compared. There were only appreciated morphometric differences between the two cultivars, with the diameter and volume of P berries and seeds (detected in integer berry) appearing significantly larger than F grapes. However, from a qualitative and morphological point of view, no relevant and reproducible differences were appreciated as a function of both p500 treatment and soil electrical conductivity.

Therefore, the next step consisted in examining hydrogen relaxation times (T_1 and T_2) and self-diffusion coefficients to obtain information on grape microstructure and on behavior, mobility and nature of the water molecules in the grapes mesocarp. Since these MRI parameters are notoriously very stable and constant, their possible and pronounced variation is diagnostic of an alteration in the tissue under examination [30]. These changes can be attributed, directly or indirectly, to factors such as: a sharp variation in the content of free water; change in microstructure and therefore in the confinement of water molecules; alteration in the consistency of the material; thickening of vascular bundles and so on [29–31].

In Fig. 8 and Sup. Table S2 are reported the results concerning T_1, T_2 and self-diffusion coefficients of F grapes. Differently than for MR images, MRI parametric data revealed singular and interesting responses depending on both p500 treatment and soil microvariability (Sup. Table S3). T_2 values ranged between 39.56 and 53.22 ms and the differences among the F types resulted statistically significant in all cases (Fig. 8a, Sup. Table S2). Even though this is only a preliminary study, it suggests the potential use of this single parameter as an innovative and diagnostic element of quality, useful to serve as supporting data to discriminate, trace and

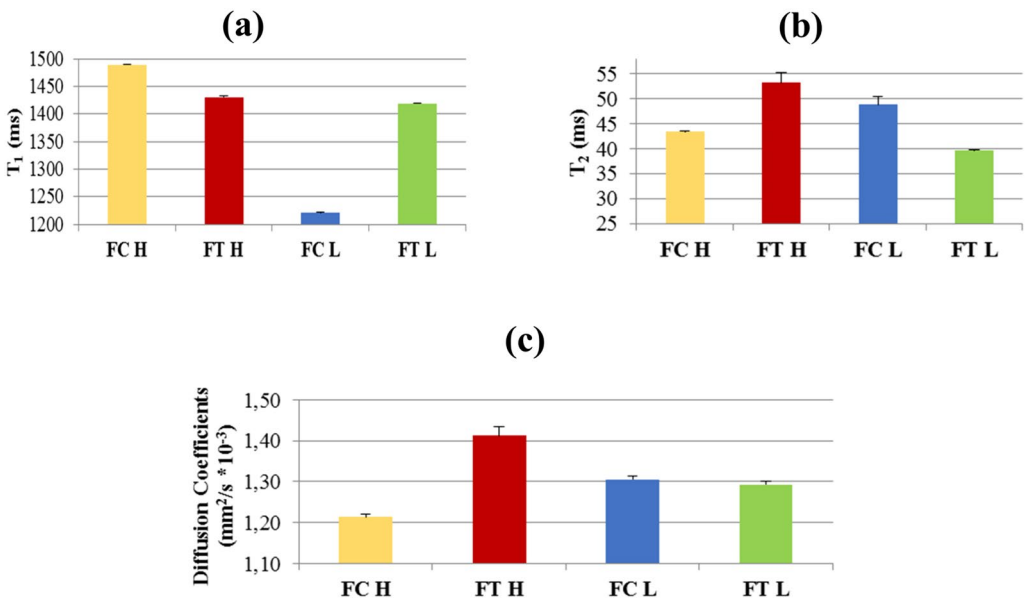

Fig. 8 Average proton longitudinal spin–lattice (T_1 in ms; **a**), transversal spin–spin (T_2 in ms; **b**) and self-diffusion coefficients (DIFF in $mm^2/s * 10^{-3}$, **c**) of Fiano grapes (control, FC, and treated, FT), collected in vineyard sites characterized by low (L) and high (H) apparent soil electrical conductivity. The bars at the top of each histograms indicate the respective standard deviation

identify grapes treated or not with preparation 500 and/or sampled from micro-areas characterized by different soil properties. Interestingly, while p500 led to the highest T_2 value, in case of high ECa values, it was detected the lowest value in case of grapes treated with p500 but sampled at soil sites with the lowest electrical conductivity. For T_1 relaxation times (Fig. 8b, Sup. Table S2), the values ranged between 1220 and 1489 ms. The T_1 values for FT_H and FT_L did not differ from each other, while a neat difference was observed between FC_H and FC_L samples, which exhibited a gap of 269 ms, with FT_H characterized by a longitudinal relaxation time of 1489 ms. Finally, the diffusion coefficients varied from 1.213 to 1.413 $mm^2/s * 10^{-3}$ (Fig. 8c, Sup. Table S2). Interestingly, the results followed a trend similar to that of T_2 results with the longest relaxation time recorded for samples collected at high ECa values and resulting from p500 treatment. For samples collected at points characterized by low ECa values, no differences were found between treated (FT_L) and untreated plants (FC_L), with values averaging around 1.3 $mm^2/s * 10^{-3}$.

Our results suggested that MRI proton relaxation times and diffusion coefficients are capable to appreciate grape structural properties and characteristics, which depend on conditions and factors affecting the vine phenological development during the fruit production. In fact, the application of p500 as well as different soil electrical conductivity were capable to induce pronounced changes in Fiano grapes, leading to relatively small but statistically significant inter-class differences (Sup. Table S3). In addition, the fact that all replicates (per berry and per ROI) exhibited a very low intra-class variance certified an excellent and promising reproducibility for such innovative analytical method. A variation in relaxation times and in water diffusivity may be explained by factors such as a change in the content and confinement of free water in the berries; alteration in the grape microstructure; development of a denser and thicker vascular system, with consequent impact on mesocarpic water mobility; modification in fruit consistency. The systematic change observed for these parameters permitted to conclude that they correlated with both p500 treatment and soil ECa, and in particular to conditions such as: (1) different bioaccessible water in soil, which directly influenced soil ECa values and indirectly the water content of the fruit, thus implying a higher dry weight; (2) a different and site-specific content of organic matter (excluding the role of active clays content which were assumed constant within the examined F vineyard); (3) the impact of the biodynamic treatment on the bioavailability of water and/or nutrients, inducing an alteration that varied depending on spatial microvariability; (4) the action of biodynamic treatment serving as a primer to shift and enrich the vine rhizospheric microbial community, with an influence on nutrient and water uptake as well as their respective physiology; (5) the greater bioavailability of iron (presumably related to the induced presence of siderophore microorganisms) capable to imply a more efficient uptake of this ferromagnetic element, known to promote an artificial shortening (i.e., not related to the tissue itself) of relaxation times. Although, at the moment, we cannot discriminate among these factors, we can assume that most of these concurred to determine the observed results as well as we can hypothesize to perform, in the future, further experiments aimed to delve deeper into these aspects. It is important to emphasize that the content in antioxidant activity and total phenols for FT_H sample resulted, absolutely, the highest. This outcome permits to infer that Fiano grapes treated with preparation 500 and developed in points characterized by relatively higher ECa values yielded grapes with a neatly superior nutraceutical quality. Consequently, we found that MRI T_2 relaxation times and diffusion coefficients of FT_H showed a similar trend, exhibiting the highest values for both parameters. This original evidence suggests that these MRI parameters may serve as indirect markers of nutraceutical quality. Consistently, the absolutely lowest value found in T_2 was that of FC_H samples, which was also the sample with the markedly poorest content in antioxidants and total phenols. Again, this finding suggests a possible correlation between nutraceutical quality of Fiano and MRI T_2.

The analytical approach conducted for Fiano grapes was attempted similarly also for Pallagrello grapes. This notwithstanding, it was not possible to obtain reliable and useful MRI data with an acceptable variance. In fact, differently than for the Fiano variety, all examined Pallagrello berries tended to collapse drastically in the MRI tube before the end of all MRI experiments (each series of MRI experiments required 8 h of continuous acquisition time) (Supporting Fig. S4). At the end of the analysis we incurred in these problems: (a) a general collapse of the entire berry, whereas in MRI analysis it is required to maintain the sample motionless throughout the whole experiments [29–31]; (b) a relevant amount of juice exuded from the berry on the bottom of the tube; (c) a greater susceptibility to pathogens attack; and (d) a drastically reduced consistency of the berry. Except for just few and not statistically relevant samples, all these conditions concurred to make Pallagrello samples (and presumably all grape varieties with similar characteristics) unsuitable for this type of MRI experiments.

Conclusions

In this work we used an innovative analytical approach to verify a possible impact exerted on grape fruit by the application of biodynamic p500 biostimulant and accounting for the vineyard spatial variability revealed by the soil electrical conductivity. We focused on two varieties of grapes very representative of the Italian excellent wine production, namely Pallagrello Nero and Fiano, and evaluated (i) the primary metabolome of grapes via HRMAS NMR; (ii) the main parameters representative of chemical and nutraceutical quality of grapes (titratable acidity; content in total phenols and polyphenols via FOLIN; content in antioxidant compounds via DPPH) (iii) grape microstructural and morphological characteristics via MRI. It is noteworthy to point out that the use of HRMAS NMR and MRI represent a relevant technological innovation. In fact, despite their indisputable ability to enable the NMR analysis of fresh and intact samples without residing into preliminary sample manipulations, they are still inexplicably unexplored and underestimated in the field of food chemistry.

This work confirmed the validity and reliability of the HRMAS technique in analyzing grape berry. In fact, permitted to detect the primary metabolome of Fiano and Pallagrello grapes, identifying the main amino acids, alcohol, organic acids, carbohydrates, and nitrogen compounds related to the primary metabolism of grapes. The elaboration of proton spectra of the different types of grapes investigated through advanced and multivariate statistical techniques proved, objectively, that the proper application of the biostimulant p500 influences the primary metabolism of plants, with effects which affetto the primary metabolism of grape. Moreover, grape berries collected in vineyard sites characterized by different ECa values exhibit a systematically different metabolome. Also chemical and nutraceutical parameters were significantly impacted by these factors. In particular, the highest nutraceutical values were recorded for Pallagrello and Fiano grapes both treated with p500 and collected at points characterized by low and high ECa values, respectively. In fact, the former contained 1.76 mg GAE/g and 3372.45 μg AAE/g, while the latter 0.89 mg GAE/g and 1717.97 μg AAE/g. Importantly, this proved that, at certain soil conditions, the biodynamic p500 may significantly improve the nutraceutical quality of this fruit.

MRI not only enabled to exam of the main structural characteristics of integer grape berries, but also permitted to extrapolate important water parametric data, such as proton relaxation times and diffusion coefficients, which were found to correlate with both p500 application and soil electrical conductivity. It was hypothesized that these variations in grape reflected the biotic and abiotic conditions experienced by the vine during the development of the examined fruit, such as different water and nutrients availability in soils, the action exerted by p500 as a primer to alter and enrich the microbial community at the rhizospheric level and so on. It is noteworthy that T_2 results showed a trend very similar with that of diffusion coefficients and that high values correlated with the highest content in total phenols and antioxidant. This outcome candidates this MRI parametric data as potential marker for grape nutraceutical quality. However, as demonstrated by the application of MRI on P grapes, a limitation of the method is that it can be applied, in a reliable way, only on grape varieties capable to remain mostly unaltered at 25 °C for at least 8 h (such as Fiano).

In conclusion, our findings have shown how the spatial microvariability of the soil and the use of p500 can affect the molecular, structural and nutraceutical characteristics of Pallagrello Nero and Fiano grapes, with effects that can presumably reflect on the quality of the resulting wines.

The proposed approach represents an efficient solution to indirectly valorize biodynamic grapes and wines. Moreover, the identified metabolomic fingerprint of p500 grapes may serve as a useful tool to help biodynamic producers to (i) promote their products via molecular traceability, (ii) contrast possible frauds and, importantly, (iii) objectively demonstrate the use of the declared biodynamic treatment.

Supplementary Information

The online version contains supplementary material available at https://doi.org/10.1186/s40538-024-00620-x.

Supplementary Material 1.

Supplementary Material 2.

Supplementary Material 3.

Acknowledgements

This work was financially supported by the Projects "modelli circolari—modelli di sistemi circolari multifunzionali per produzioni tipiche (MIPAAF)" and "Spettroscopie NMR HRMAS e MRI per correlare, rispettivamente, il metaboloma primario e parametri strutturali di uva Fiano e Pallagrello nero all'azione di biostimolanti e alla conducibilità elettrica apparente del suolo del vigneto (University of Salerno—orsa230438)".

Author contributions

P.M. contributed to conceptualization, methodology, formal analysis, investigation, resources, manuscript editing, supervising and reviewing and funding acquisition. A. S. and C.M. contributed to formal analysis, investigation, original draft of the manuscript. N. F. contributed to formal analysis and investigation. S. De P. and A.P. contributed to conceptualization and manuscript reviewing. G. C. contributed to conceptualization, investigation, resources, manuscript reviewing and funding acquisition.

Funding

Not applicable.

Availability of data and materials
Not applicable.

Declarations

Ethics approval and consent to participate
Not applicable.

Consent for publication
Not applicable.

Competing interests
The authors declare that they have no competing interests.

Author details
[1]Department of Pharmacy, University of Salerno, Via Giovanni Paolo II, 132, Fisciano, Italy. [2]Department of Physics, University of Salerno, Via Giovanni Paolo II, 132, Fisciano, Italy. [3]Department of Agriculture, University of Naples "Federico II", Via Università 100, Portici, Italy.

Received: 30 April 2024 Accepted: 18 July 2024
Published online: 06 September 2024

References

1. Khan N, Fahad S, Faisal S, Naushad M. Grape production critical review in the world. SSRN Electron J. 2020. https://doi.org/10.2139/ssrn.3595842.
2. Vinci G, Prencipe SA, Abbafati A, Filippi M. Environmental impact assessment of an organic wine production in central Italy: case study from Lazio. Sustainability. 2022;14(22):15483.
3. Dordevic N, Wehrens R, Postma GJ, Buydens LMC, Camin F. Statistical methods for improving verification of claims of origin for Italian wines based on stable isotope ratios. Anal Chim Acta. 2012;757:19–25.
4. Pereira GE, Gaudillere J-P, Pieri P, Hilbert G, Maucourt M, Deborde C, Moing A, Rolin D. Microclimate influence on mineral and metabolic profiles of grape berries. J Agric Food Chem. 2006;54(18):6765–75.
5. Asselin C, Morlat R, Barbeau G. Le Terroirs Viticoles: du concept au produit. Terroir, Zonazione, Viticoltura. Phytoline ED, Rivoli Veronese (VR). 2003. p. 159–86.
6. Bulgari R, Franzoni G, Ferrante A. Biostimulants application in horticultural crops under abiotic stress conditions. Agronomy. 2019;9:306.
7. Tangolar S, Tangolar S, Canturk S. The role of biostimulants in viticulture. In: Current agricultural studies in Türkiye: research and reviews. Ankara: IKSAD Publishing House; 2022. p. 203–27.
8. Fallahi HR, Taherpour R, Aghhavani-Shajari M, Soltanzadeh MG. Effect of super absorbent polymer and deficit irrigation on water use efficiency, growth and yield of cotton. Not Sci Biol. 2015;7(3):338–44.
9. Bernardo S, Dinis LT, Machado N, Moutinho-Pereira J. Grapevine abiotic stress assessment and search for sustainable adaptation strategies in Mediterranean-like climates. A review. Agron Sustain Dev. 2018;38(6):1–20.
10. Vazquez-Rowe R, Moreira MT, Villanueva-Rey P, Feijoo G. Comparative life cycle assessment in the wine sector: biodynamics vs conventional viticulture activities in NW Spain. J Clean Prod. 2013;65:330–41.
11. Steiner R. Agriculture: a course of eight lectures. London: Biodynamic Agricultural Association; 1972.
12. Spaccini R, Mazzei P, Squartini A, Giannattasio M, Piccolo A. Production of the BD preparation 500, molecular properties of a fermented manure preparation used as field spray in biodynamic agriculture. Environ Sci Pollut Res. 2012;19:4214–25.
13. Reeve JR, Carpenter-Boggs L, Reganold JP, York AL, Brinton WF. Summary and conclusion, influence of biodynamic preparations on compost development and resultant compost extracts on wheat seedling growth. Bioresour Technol. 2010;5665:5658–66.
14. Picone G, Trimigno A, Tessarin P, Donnini S, Rombolà AD, Capozzi F. ^{1}H NMR foodomics reveals that the biodynamic and the organic cultivation managements produce different grape berries. Food Chem. 2016;213:187–95.
15. Davis JG, Kitchen NR, Sudduth KA, Drummond ST. Using electromagnetic induction to characterize soils. Better Crops; 1997. p. 6–8.
16. Doolitle JA, Brevik EC. The use of electromagnetic induction techniques in soils studies. Geoderma. 2014;223:33–45.
17. Misra RK, Padhi J. Assessing field-scale soil water distribution with electromagnetic induction method. J Hydrol. 2014;516:200–9.
18. Lardo E, Coll P, Le Cadre E, Palese AM, Villenave C, Xiloyannis C, Celano G. Electromagnetic induction (EMI) measurements as a proxy of earthworm presence in southern France vineyard. Appl Soil Ecol. 2012;61:76–84.
19. Lardo E, Palese AM, Nuzzo V, Xiloyannis C, Celano G. Variability of total soil respiration in a Mediterranean vineyard. Soil Res. 2015;53:531–41.
20. Stadler A, Rudolph S, Kupisch M, Langensiepen M, Van der Kruk J, Ewert F. Quantifying the effects of soil variability on crop growth using apparent soil electrical conductivity measurements. Eur J Agron. 2015;64:8–20.
21. Rudolph S, Wongleecharoen C, Lark RM, Marchant BP, Garré S, Herbst M, Weihermuller L. Soil apparent conductivity measurements for planning and analysis of agricultural experiments: a case study from western-Thailand. Geoderma. 2016;267:220–9.
22. Mazzei P, Celano G, Palese AM, Lardo E, Drosos M, Piccolo A. HRMAS-NMR metabolomics of Aglianicone grapes pulp to evaluate terroir T and vintage effects, and as assessed by the electromagnetic induction (EMI) technique, spatial variability of vineyard soils. Food Chem. 2019;216:215–23.
23. Doty FD, Entzminger G, Yang AY. Magnetism in high-resolution NMR probe design. II: HR MAS. Concepts Magn Reson Educ J. 1998;10:239–60.
24. Mazzei P, Piccolo A. HRMAS NMR spectroscopy applications in agriculture. In: Chemical and biological technologies in agriculture. Heidelberg: Springer; 2017. p. 1–13.
25. Mazzei P, Piccolo A, Valentini M. Intact food analysis by means of HRMAS-NMR spectroscopy. In: Webb GA, editor. Modern magnetic resonance. Cham: Springer; 2017. p. 1–16.
26. Mazzei P, Vinale F, Woo SL, Pascale A, Lorito M, Piccolo A. Metabolomics by proton high-resolution magic-angle-spinning nuclear magnetic resonance of tomato plants treated with two secondary metabolites isolated from trichoderma. J Agric Food Chem. 2016;64:3538–45.
27. Santos ADDC, Fonseca FA, Dutra LM, Santos MFC, Menezes LRA, Campos FR, Nagata N, Ayub R, Barison A. ^{1}H HR-MAS NMR-based metabolomics study of different persimmon cultivars (*Diospyros kaki*) during fruit development. Food Chem. 2018;239:511–9.
28. Ritota M, Marini F, Sequi P, Valentini M. Metabolomic characterization of Italian sweet pepper (*Capsicum annum* L.) by means of HRMAS-NMR spectroscopy and multivariate analysis. J Agric Food Chem. 2010;58(17):9675–84.
29. Mazzei P, et al. High-resolution magic-angle-spinning NMR and magnetic resonance imaging spectroscopies distinguish metabolome and structural properties of maize seeds from plants treated with different fertilizers and arbuscular mycorrhizal fungi. J Agric Food Chem. 2018;66(11):2580–8.
30. Hills B. Magnetic resonance imaging in food science. New York: Wiley; 1998.
31. Mannina L, Mazzei P, et al. Spettroscopia in Risonanza Magnetica Nucleare nelle scienze degli alimenti. Zanichelli. 2023.
32. Mannina L, Sobolev A, Proietti M, Capitani D, Mazzei P, Piccolo A, et al. NMR methodologies in food analysis. In: Analytical chemistry: developments, applications, and challenges in food analysis. New York: Nova Science Publishers, Inc.; 2017. p. 103–56.
33. Valentini M, Sequi P, Ciampa A, Ritota M, Taglienti A, Cozzolino S, Conte L, Terlizzi M. Qualità tramite Risonanza Magnetica per Immagini: valutazione della conservazione e dei trattamenti agronomici. Italus Hortus. 2009;16(5):324–8.
34. Sequi P, Dell'Abate MT, Valentini M. Identification of cherry tomatoes growth origin by means of magnetic resonance imaging. J Sci Food Agric. 2007;87:127–32.
35. Ciampa A, Dell'Abate MT, Masetti O, Valentini M, Sequi P. Seasonal chemical–physical changes of PGI Pachino cherry tomatoes detected by magnetic resonance imaging (MRI). Food Chem. 2010;122:1253–60.
36. Salerno A, Pierandrei F, Rea E, Sequi P. Definition of internal morphology and structural changes due to dehydration of radish (*Raphanus sativus* L. cv Suprella) using magnetic resonance imaging spectroscopy. J Food Qual. 2005;28:428–38.

37. Taglienti A, Sequi P, Cafiero C, Cozzolino S, Ritota M, Ceredi G, Valentini M. Hayward Kiwifruits and plant growth regulators: detection and effects in post-harvest studied by magnetic resonance imaging and scanning electron microscopy. Food Chem. 2011;126(2):731–6.
38. Kerr WL, Clark CJ, McCarthy MJ, de Ropp JS. Freezing effects in fruit tissue of kiwifruit observed by magnetic resonance imaging. Sci Hortic. 1997;69:169–79.
39. Wang SY, Wang PC, Faust M. The non-destructive detection of watercore in apple with nuclear magnetic resonance imaging. Sci Hortic. 1988;35:227–34.
40. Clark CJ, MacFall JS, Bieleski RL. Loss of watercore from 'Fuji' apple observed by magnetic resonance imaging. Sci Hortic. 1998;73:213–27.
41. Melado Herreros A, Munoz-García MA, Blanco A, Val J, Fernandez Valle ME, Barreiro Elorza P. Relationship between solar radiation on watercore on apple fruit assessed with MRI. In: International conference of agricultural engineering. 2012. p. 1–5.
42. Jacobsen NE. NMR spectroscopy explained—simplified theory, applications and examples for organic chemistry and structural biology. Spin Echo Att Proton Test. 2007.
43. Brereton RG, Wiley J & Sons. Chemometrics: data analysis for the laboratory and chemical plant. J Anal Chem Engl. 2003;60:183–249.
44. Worley B, Powers R. Multivariate analysis in metabolomics. Curr Metabolomics. 2013;1:92–107.
45. Mulas G, Galuffi MG, Pretti L, Nieddu G. NMR analysis of seven selections of Vermentino grape berry: metabolites composition and development. J Agric Food Chem. 2011;59:793–802.
46. Hong YS. NMR-based metabolomics in wine science. Magnet Res Chem. 2011;49:13–21.
47. Botelho RV, Roberti R, Tessarin P, Garcia-Mina JM, Rombolà AD. Physiological responses of grapevines to biodynamic management. Renew Agric Food Syst. 2016;31(5):402.
48. Sansavini S, Costa G, Gucci R, Inglese P, Ramina R, Xiloyannis C. Forme di allevamento e potatura della vite, Arboricoltura generale. Granarolo dell'Emilia: Patron editori Bologna; 2012. p. 383–6.
49. Sicheri G. Le principali caratteristiche botaniche dell'uva. Il libro completo del Vino, 16A edizione, DeAgostini. 2017. p. 34–35(34–48).
50. Tartian AC, Cotea V, Niculaua M, Zamfir CI, Colibaba CL, Morosanu AM. The influence of the different techniques of maceration on the aromatic and phenolic profile of the Busuioaca de Bohotin wine. In: Bio web of conferences. 2017.
51. Cherviak SN, Anikina NS, Gnilomedova NV, Gnilomediva VG, Gerzhikova VG, Vesiutova AV. Study of physic-chemical and biochemical parameters of technical varieties of grapes. Earth Environ Sci. 2021;659: 012087.
52. Zhang P, Needs S, Liu D, Fuentes S. The influence of apical and basal defoliation on the canopy structure and biochemical composition of *Vitis vinifera* cv. Shiraz grapes and wine. Front Chem. 2017;5:1–9.
53. Ramirez-Lopez LM, DeWitt CAM. Analysis of phenolic compounds in commercial dried grape pomace by high-performance liquid chromatography electrospray ionization mass spectrometry. Food Sci Nutr. 2014;2:470–7.
54. Cadota Y, Minana Castello MT, Chevalier M. Flavan-3-ol compositional changes in grape berries (*Vitis vinifera* L. cv Cabernet Franc) before veraison, using two complementary analytical approaches, HPLC reversed phase and histochemistry. Anal Chim Acta. 2006;563:65–75.
55. Ivanova V, Stefova M, Vojnoski B, Dornyei A, Mark L, Dimovska V, Stafilov T, Kilar F. Identification of polyphenolic compounds in red and white grape varieties grown in R. Macedonia and changes of their content during ripening. Food Res Int. 2011;44:2851–60.
56. Derradji-Benmeziane F, Djamai R, Cadot Y. Antioxidant capacity, total phenolic, carotenoid, and vitamin C contents of five table grape varieties from Algeria and their correlations. OENO One. 2014;48(2):153–62.
57. Montero GC, Minatel IO, Junior AP, Alonzo Gomez H, Correa de Camargo JP, et al. Bioactive compounds and antioxidant capacity of grape pomace flours. LWT. 2021;135: 110053.
58. Ciampa A, Dell'Abate MT, Florio A, Tarricone L, Di Gennaro D, Picone G, Trimigno A, Capozzi F, Benedetti A. Combined magnetic resonance imaging and high-resolution spectroscopy approaches to study the fertilization effects on metabolome, morphology and yeast community of wine grape berries, cultivar Nero di Troia. Food Chem. 2019;274:831–9.

Publisher's Note

Springer Nature remains neutral with regard to jurisdictional claims in published maps and institutional affiliations.